Water and Environmental Research Center
Annual Technical Report
FY 2004

Introduction

The Water and Environmental Research Center (WERC) at the University of Alaska Fairbanks (UAF) is presently housed in the Institute of Northern Engineering (INE). INE is the research arm of the newly created College of Engineering and Mines (CEM), where the Director of WERC reports directly to the Director of INE. The Water and Environmental Center continues to prosper and grow. At present, the basic USGS 104B grant program represents between 3 and 4 % of WERCs total annual budget. Currently there are about 12 faculty that are very active in WERC and about 6 that have minor roles. There are over 30 graduate students; about 20 % are PhD students. An additional ten professional people fill various technical research support functions.

Research needs across the State with three major climate zones (maritime, continental and arctic) are quite diverse and variable. Resource development drives much of the required research. High demand for water in concentrated areas (such as oil development in the Arctic) is an important challenge. Also, the high latitude position of Alaska with the projected amplification of global warming has made Alaska an excellent natural research observatory to document change. Issues of integrated water, wastewater, power and heating systems for rural villages are always an ongoing challenge. WERC faculty derive 54 % of their research dollars from federal agencies (NSF, DOE, NASA, USFS, EPA, NOAA etc.), 10 % from private sources, 29 % from the state and the remainder from a variety of sources.

Faculty, staff and students in WERC continue to be very active in communicating their research results to the various scientific communities and public. This is done through a variety of venues from technical conferences (ASCE, AGU, AWRA, etc.) to presentations in villages and K-12. Results are also distributed on our website (http://www.uaf.edu/water/) and through an electronic newsletter (http://www.uaf.edu/ine/researchflash.htm). On the WERC website are also hydrological and meteorological data (near real time) from about 40 field sites distributed around the state. This data is made available for use by others.

Research Program

During the research year 2004-2005 (March 1, 2004 to February 28, 2005), four projects were funded through the USGS 104B program. Since these grants are relatively small in size, they are primarily used for graduate student support and to help young faculty initiate new research. The cost per student is about $31,000 (stipend plus tuition) per year. This allocation allows us to fund between three to four research projects (most years some additional funds are added from outside sources to increase the total funds available.

The four funded projects are:

"Short- and Long-term As-aluminum Oxyhydroxide Sorption Interactions in Aquatic and Soil Environments", by Drs. Silke Schiewer and Paras Trivedi

"Monitoring Thermokarst Evolution at Caribou-Poker Creeks Research Watershed", by Dr. Horacio Toniolo

"Development of Crab Shell Based Biosorbents to Remove Anionic Heavy Metal Complexes from Contaminated Water", by Dr. Silke Schiewer

"Short- and Long-term As-aluminum Oxyhydroxide Sorption Interactions in Aquatic and Soil Environments", by Drs. Silke Schiewer and Paras Trivedi

"Investigation of the Formation of Pore Ice in Coarse Grained Soils", by Drs. David L. Barnes and Yuri Shur

Short- and Long-term As-Aluminium Oxyhydroxide Sorption Interactions in Aquatic and Soil Environments

Basic Information

Title:	Short- and Long-term As-Aluminium Oxyhydroxide Sorption Interactions in Aquatic and Soil Environments
Project Number:	2004AK21B
Start Date:	3/1/2004
End Date:	3/1/2005
Funding Source:	104B
Congressional District:	AK
Research Category:	Water Quality
Focus Category:	Toxic Substances, Geochemical Processes, Treatment
Descriptors:	arsenic, sorption, aluminum hydroxide, XAS
Principal Investigators:	Silke Schiewer, Paras Ishvarlal Trivedi

Publication

1. Tanwar, K.; Trivedi, P.; Schiewer, S.: A multi-scale assessment of As(V)-aluminium oxyhydroxide interactions. 2005. In: Proceedings of ASCE EWRI World Water & Environmental Resources Congress, Anchorage, AK, May 15-19 (12 pp.).
2. Tanwar, K.; Schiewer, S.; Trivedi, P.: A multi-scale assessment of As(V)-aluminium oxyhydroxide interactions. 2005. In: Abstracts of ASCE EWRI World Water & Environmental Resources Congress, Anchorage, AK, May 15-19.
3. Tanwar, K.; Trivedi, P.; Schiewer, S.; Pandya, K.: Long-term kinetics of As(V)-aluminum oxyhydroxides interactions: complementing macroscopic results with spectroscopic analyses. 2004. In: Advances in environmental reaction kinetics and thermodynamics: long-term fate of anthropogenic contaminants. Abstracts of the 228th Annual Meeting, American Chemical Society (ACS), Philadelphia, August 22-26.

Problem and research objectives

Arsenic has emerged as a major threat to global sustainability during the last decade. In aquatic and soil environments, arsenic results from natural weathering of minerals as well as from anthropogenic activities, such as mining and wood preservation. In most natural systems, arsenate (As(V)) is the predominant form of As from all of these sources. However, in reducing conditions, arsenic is present in reduced forms, such as arsenite.

Arsenic exposure to human beings can result in acute and chronic health effects such as cancer. Based on recommendations from several ecotoxicological and risk assessment studies, U.S. EPA announced lowering the maximum contaminant level (MCL) for As in drinking water to 10 ppb effective 2006. This new stringent standard emphasizes the need to improve the capability of current environmental models to accurately predict the long term mobility and bioavailability of As in aqueous and soil ecosystems. Therefore, the understanding of As speciation is very critical for accurate risk assessment.

The objective of this research was to study As(V) sorption onto hydrous aluminum oxides (HAO) under traditional boundary conditions as well as continuous As(V) influx conditions. Furthermore, As(V)-HAO interactions were also studied in presence of phosphate to study the effect of oxyanions on As(V) sorption. For this purpose, macroscopic studies were conducted and modeled after determining parameters, such as equilibrium constant (K) and maximum sorption capacity (C_t). However, to predict the long term fate of As(V) in nature, a molecular scale understanding of its interactions with environmentally relevant sorbents is necessary. Therefore, to elucidate the fundamental reaction mechanism at the oxide surface, macroscopic studies are complemented with XAS.

Methodology

All experiments used American Chemical Society (ACS) reagent grade chemicals and double-deionized water. Experiments were performed at 25^oC, under closed system conditions (N_2 glove box) to avoid interference from reactive gases, such as carbon dioxide (CO_2) and methane (CH_4). Turbulent hydraulic conditions ($Re \geq 10^5$, with respect to length of reactor) were used to minimize external mass-transfer resistances (Fogler, 2002).

Synthesis and Characterization of HAO

HAO was precipitated according to a modified method of Gadde and Laitinen (1974) (Trivedi and Axe, 1999). Prior to sorption studies, all HAO suspensions were repeatedly centrifuged and washed with double deionized water and then finally aged for 24 h at an adjusted ionic strength (I.S.) of 10^{-2} M $NaNO_3$.

Sorption Studies

All As(V)-HAO sorption studies were conducted using 1 g L^{-1} HAO suspension, at pH 4.5 ± 0.2, and background I.S. 10^{-2} M $NaNO_3$. The stock solution of As(V) was prepared using sodium arsenate ($Na_2HAsO_4 \cdot 7H_2O$) and stored at pH 4.5 in a nitrogen glove box. All arsenate sorption studies were conducted in 1-L HDPE containers, where the bulk aqueous pH was monitored and maintained using a Brinkmann autotitrator (799 GPT Titrino). Preliminary kinetic studies suggested that a contact time of 4 h is sufficient for equilibration of As(V) sorption on the

external surface of HAO. As a result, all isotherm studies were conducted using a reaction time of 4 h for a concentration range of 5×10^{-6} - 5×10^{-3} M of As(V). The effect of competing oxyanions on the sorption of As(V) was studied by allowing equimolar amounts of arsenate and phosphate to react with HAO.

Long-term kinetics of As(V)-HAO interactions were conducted under two different sets of boundary conditions. In the first set, traditional boundary conditions (TBC) were employed, where 10^{-3} M of As(V) was initially added to the HAO suspension and the sorptive uptake was measured as a function of reaction time up to 360 h. Under these conditions, the concentration gradient, which is the primary driving force for the sorption reactions, quickly decreases with time. Continuous influx condition (CIC) experiments were also conducted. In these experiments, a continuous driving force was maintained by adding 10^{-5} M As(V) every 4 h using a dual probe autotitrator (Brinkmann 799 GPT Titrino), which also monitored and maintained the system pH constant at 4.5, over a contact time of 400 h.

Samples collected from all sorption studies were filtered using 0.2 μm membrane filters. Aqueous arsenic concentrations in these filtrates were measured using graphite furnace atomic absorption (GAA) spectrometer (Perkin-Elmer Analyst 800) (Deaker et al., 1999).

XAS Studies

The local coordination of As(V) in the sorption complexes was studied as a function of reaction time, sorbate loading, and the presence or absence of phosphate using x-ray absorption spectroscopy (XAS). All XAS studies were conducted on beamline X11B at National Synchrotron Light Source (NSLS), Brookhaven National Laboratory, where the maximum storage ring beam energy was 2.8 GeV with a maximum beam current of 280 mA. To compare and identify the local structure of As in the sorption complexes, XAS spectra were also collected for the following arsenic references: $As_2O_5(s)$, $As_2O_3(s)$, and a 10^{-1} M aqueous sodium arsenate solution at pH 4.5. Multiple scans were collected for each sample to improve signal-to-noise ratio. Details in experimental methodology and data evaluation are described in Tanwar et al. (2005).

Principal findings and significance

Sorption Studies

The results obtained from the isotherm studies show (Figure 1a) a linear correlation between the moles of As(V) sorbed g^{-1} HAO and the bulk aqueous As(V) concentration at lower concentrations. At higher concentrations, the isotherm approaches a plateau, which represents saturation of sorption sites available on the external surface and as well as on the macropore walls of HAO. The isotherm was modeled using the single site Langmuir isotherm model. This model assumes one type of reaction sites, monolayer coverage, and no change in affinity with sorption density (Fogler, 2002).

As shown in Figure 1a, this model satisfactorily fits experimental data. The estimated maximum sorption capacity (C_t) of HAO for As(V) is 1.9×10^{-3} mol g^{-1} HAO (within 21% standard deviation) and the equilibrium constant (K) is approximately 4.5×10^3 L mol^{-1} (within 21% standard deviation). Anderson et al. (1976) reported the maximum sorption capacity for As(V) as 1.6×10^{-3} mol g^{-1} on amorphous aluminum oxide at pH 5, which is slightly lower than

that found in the present study. The higher sorption capacity achieved in the present study can be attributed to lower pH used in this study, which would result in higher net positive charge on the oxide surface, and therefore in a high apparent capacity for oxyanions such as As(V).

The isotherm experiments conducted in presence of phosphate were also modeled using the same single-site Langmuir isotherm model. For modeling this isotherm, the equilibrium constant was constrained as equal to the value estimated in single system studies; The isotherm modeling for this study is presented in Figure 1b. The modeling results reveal that the sorption capacity for As(V) sorption on HAO is 1.6×10^{-3} mol g^{-1} (within 21% standard deviation) in presence of phosphate as compared to the single sorbate system, where it is approximately 1.9×10^{-3} mol g^{-1} (within 21% standard deviation). These results indicate that sorption capacity of HAO for As(V) decreased slightly due to presence of phosphate. However, this decrease seems insignificant if associated errors are considered.

To obtain information about the rate limiting step, long-term As(V) sorption was studied over a reaction time of 400 h, under different mass-transfer conditions. The time dependence of As(V) sorption onto HAO under two different mass transfer conditions, i.e. one time addition (TBC) and continuous supply (CIC), is presented in Figures 2a and 2b, respectively. A total of 10^{-3} moles As(V) was added to the reaction system in both TBC and CIC studies. In TBC studies, approximately 8.7×10^{-4} mol As(V) was sorbed g^{-1} HAO after reaction time of 4 h and no significant increase in uptake of As(V) was observed after the reaction time of 4 h until 300 h (Figure 3a).

Under similar mass transfer conditions, Arai et al. (2001) observed an increase in As(V) uptake from 1.9×10^{-4} to 2.0×10^{-4} mol g^{-1} γ-Al_2O_3 with increase in reaction time from 72-8760 h. Likewise, Fuller et al. (1993) observed rapid uptake of As(V) on ferrihydrite within the first 4 h followed by a very slow uptake till a reaction time of 200 h. Although the magnitude of increased uptake in these studies appears insignificant, it indicates that the process following rapid initial adsorption is very slow and might take months to years to reach equilibrium. Therefore, it is difficult to asses the contribution of such slow processes under these conditions.
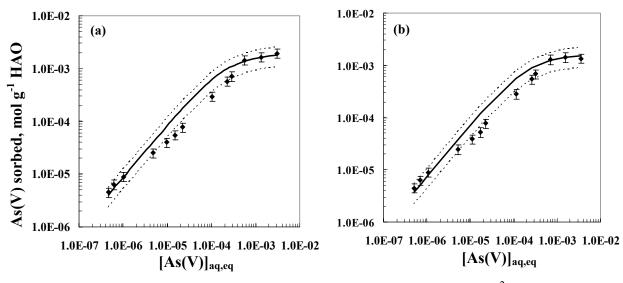
Figure 1. Arsenate adsorption isotherms conducted at 25°C, pH 4.5, I.S. 10^{-2} M. Solid lines represent the single site Langmuir mode, dashed lines show the associated errors of ± 2 SD

(a) in absence of phosphate;
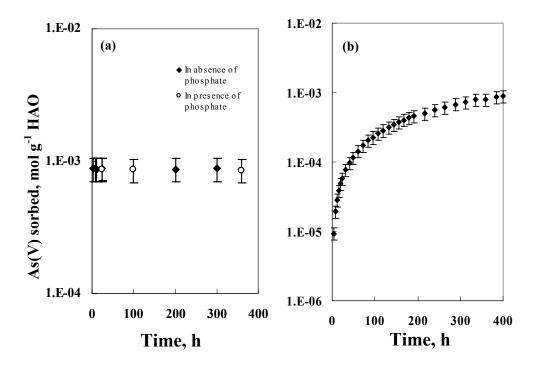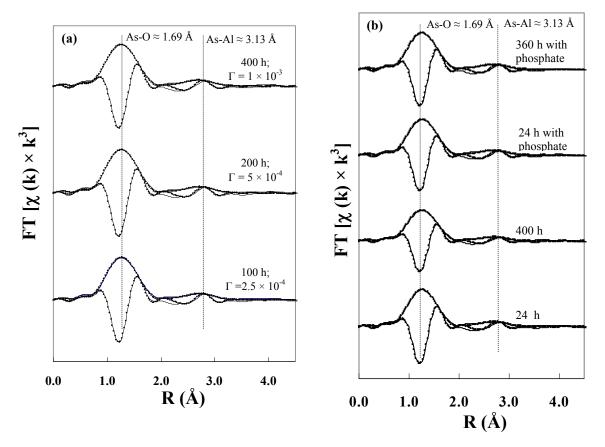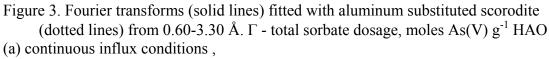(b) in presence of phosphate in equimolar amount with As(V).

Figure 2. Long-term kinetic studies of As(V) sorption on HAO (pH 4.5, I.S. 10^{-2} M)
(a) Traditional boundary conditions, in absence and presence of equimolar phosphate
(b) Continuous influx conditions, 10^{-5} M As(V) supplied every 4 h.

Figure 3. Fourier transforms (solid lines) fitted with aluminum substituted scorodite (dotted lines) from 0.60-3.30 Å. Γ - total sorbate dosage, moles As(V) g^{-1} HAO
(a) continuous influx conditions ,
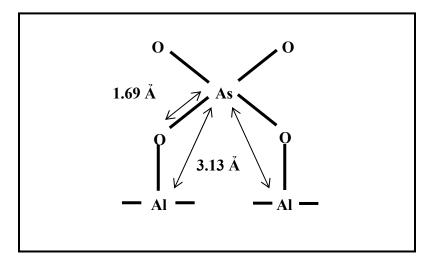(b)traditional boundary conditions.

Figure 4 Local structure of As(V)-HAO sorption complexes based on XAS results. As-O $\approx$ 1.69 Å and As-Al $\approx$ 3.13 Å.

To maintain a continuous concentration gradient of As(V), continuous influx condition (CIC) studies were conducted, where 10^{-5} M of As(V) were added every 4 h to the reaction system, over a reaction time of 400 h. Unlike TBC studies, the results of this study reveal that there was a rapid uptake until a reaction time of 24 h, and a slow but continuous uptake until the reaction time of 400 h (Figure 2b). Additionally, a slightly higher uptake of As(V) (8.9×10^{-4} mol As(V) g^{-1} HAO) was observed in CIC studies as compared to TBC studies. The final concentration of As(V) in bulk solution was approximately 1.1×10^{-4} M at the end of 400 h. This difference can be qualitatively explained in terms of maintaining a driving force for diffusion and the porous nature of HAO. In TBC studies, where the sorbate is supplied only once, the initial sorption is predominantly on surface sites. With increase in reaction time, the sorbate may start migrating to pore walls of HAO. This migration would vacate few external reaction sites, where further uptake of sorbate is possible. But this process is likely to be slow and therefore, no significant increase in uptake due to diffusion can be detected within the time frame of this study. In comparison, sorbate was continuously re-supplied in CIC studies. The re-supplied sorbate is likely to occupy the external surface sites that are previously unoccupied as well as the sites that are vacated due to migration of sorbate to pore walls of HAO. In other words, the total sorption in CIC studies has contribution from sorption to external sites as well as uptake into pore walls due to intra-particle diffusion. Thus, the results of the present study suggest that intra-particle diffusion could be the predominant rate limiting step in case of long-term studies, which further indicates that intra-particle diffusion may be an important process that controls the long-term fate of As(V) in environment.

Another important factor that can impact sorption of As(V) is the presence of competing oxyanions. The sorption studies conducted in presence of phosphate revealed that an equimolar amount of phosphate did not affect As(V) sorption over a reaction time of 360 h (Fig 2a). In comparison, Jain et al. (2000) suggested that the presence of an equimolar amount of phosphate reduced the sorption of As(V) by 0.7 % at pH 4 on ferrihydrite; however the associated errors were not reported. Therefore, this small change is likely insignificant. In contrast, Liu et al. (2001) reported that the sorption capacity of goethite for As(V) decreased from 1.8×10^{-4} to 1.1×10^{-4} mol g^{-1} due to the presence of an equimolar amount of phosphate at pH 4.0. However, the results of the present study suggest that the effect of an equimolar amount of phosphate on arsenate sorption on HAO is insignificant at pH 4.5.

XAS Studies

The XAS results are used to determine the nature of As(V)-HAO sorption complexation reactions as a function of contact time, sorbate loadings, and different mass transfer conditions (TBC and CIC). The fourier transforms and fits are presented in Figures 3a and 3b. For all sorption samples, the best fit first shell suggested approximately four oxygen atoms at an average radial distance of 1.69 ± 0.02 Å. Similar As-O distances were observed with other sorbents.

The best fits revealed that the second shell has two Al atoms at an average radial distance of 3.13 ± 0.05 Å. These As-Al distances and coordination numbers do not resemble Al-substituted scorodite, which has four Al in second shell with distances ranging from 3.34-3.38 Å. Thus, the precipitation or solid solution resulting in formation of $AlAsO_4$ can be considered insignificant. Furthermore, inclusion of As and/or O in the second shell of As(V) sorbed onto HAO, in absence or presence of Al atoms, did not provide reasonable fits. This suggests that there are no As-As interactions in the sorption complexes. The lack of these interactions validates the assumption of the Langmuir isotherm that there are no sorbate-sorbate interactions. The coordination numbers and bond distances obtained from EXAFS results of this study suggest that As(V) appears to react with HAO to predominantly form bidentate inner sphere complexes (Figure 4), where there is no interaction between the sorbed arsenate species.

The long-term stability of these sorption complexes plays an important role in determining the predominant reaction mechanism. Interestingly, the local coordination of As(V) sorbed onto HAO, under traditional as well as constant boundary conditions, did not change between 24 and 400 h of contact time. In the present study, the coordination of the sorption complexes did not vary with sorbate/sorbent ratios, over three orders of magnitude of sorbate concentration (10^{-4}-10^{-2} M As(V)), under either of the two (one time addition and continuous supply of As(V)) reaction conditions. Since no change in sorption mechanism occurred, one can reasonably attribute the continued uptake of arsenate by HAO to the slow migration of As(V) inside the micro- and/or nano-pores of these oxides, where the sorption sites are apparently similar to those located on the external surfaces as well on the macropore walls of HAO.

The local coordination and structure of sorption samples prepared in absence and presence of phosphate show a strong resemblance. This similarity suggests that equimolar amounts of phosphate has little to no influence on As(V)-HAO reaction mechanisms over a reaction time of 360 h at pH 4.5. Thus, these spectroscopic results validate the modeling of binary system isotherms using a Langmuir isotherm model with the equilibrium constant estimated from single system studies.

Conclusions

Overall, the macroscopic and spectroscopic analyses conducted in this study provide a few important conclusions. Most importantly, As(V) chemisorbs onto HAO, via one average reaction mechanism over a wide range of sorbate/sorbent ratios resulting in bidentate inner-sphere complexes.

This, in turn, justifies fitting of As(V)-HAO adsorption isotherms with a single-site Langmuir isotherm model to obtain a unique equilibrium constant and a maximum sorption capacity at constant pH.

Importantly, the sorption capacity of HAO for As(V) was not affected by the presence of phosphate in equimolar amount with As(V). Additionally, for a given set of sorbate/sorbent ratio, pH, and temperature, the structure of As(V)-HAO complexes does

not vary with time and/or presence other background oxyanions, such as phosphate, which is indicative of their chemical stability.

Furthermore, since no change in mechanism occurred over time, the slow and continuous uptake of As(V) by microporous HAO for continuous As supply can be attributed to intraparticle diffusion, where the sorption reaction mechanism along the micro- and nano-pore walls is similar to the one on the external surface. Thus, microporous oxyhydroxides of aluminum are much larger sinks for oxyanions, such as As(V), than presently understood.

References

Arai, Y.; Elzinga, E.; Sparks, D. (2001) X-ray absorption spectroscopic investigation of arsenite and arsenate adsorption at the aluminum oxide-water interface. *Journal of Colloid and Interface Science*, 235, 80-88.

Deaker, M.; William, M. (1999) Determination of arsenic in arsenic compounds and marine biological tissues using low volume microwave digestion and electrothermal atomic absorption spectrometry. *Journal of Analytical Atomic Spectrometry*, 14, 1193-1207.

Fogler, H. (2002) Elements of Chemical Reaction Engineering, 3rd ed.; Prentice Hall India: New Delhi.

Fuller, C.; Davis, J.; Waychunas, G. (1993) Surface chemistry of ferrihydrite: Part 2. Kinetics of arsenate adsorption and coprecipitation. *Geochimica et Cosmochimica Acta*, 57, 2271-2282.

Jain, A.; Loeppert, R. (2000) Effect of competing anions on the adsorption of arsenate and arsenite by ferrihydrite. *Journal of Environmental Quality*, 29, 1422-1430.

Liu, F.; De C.; Violante, A. (2001) Effect of pH, phosphate and oxalate on the adsorption/desorption of arsenate on/from goethite. *Soil Science*, 166, 197-208.

Tanwar, K.; Trivedi, P.; Schiewer, S.: An assessment of arsenic-aluminium oxyhydroxide interactions under different mass-transfer conditions relevant to natural environments. In: Proceedings of ***ASCE EWRI World Water & Environmental Resources Congress***, Anchorage, AK, May 15-19 2005 (12 pp.).\

Trivedi, P.; Axe, L. (1999) A comparison of strontium sorption to hydrous aluminum, iron, and manganese oxides. *Journal of Colloid and Interface Science*, 218, 554-563.

Monitoring Thermokarst Evolution at Caribou-Poker Creeks Research Watershed

Basic Information

Title:	Monitoring Thermokarst Evolution at Caribou-Poker Creeks Research Watershed
Project Number:	2004AK25B
Start Date:	3/1/2004
End Date:	3/1/2005
Funding Source:	104B
Congressional District:	AK
Research Category:	Ground-water Flow and Transport
Focus Category:	Hydrology, None, None
Descriptors:	thermokarst, discharge, suspended sediment concentration, bed sediment transport, mapping
Principal Investigators:	Horacio Toniolo

Publication

1. Kodial, P. Toniolo, H., Hinzman, L. & Yoshikawa, K. 2005. Thermokarst evolution in sub-arctic Alaska: A study case. In Proceedings: World Water & Environmental Resources Congress, May 15-20, 2005, Anchorage, AK. 11 pps.
2. Toniolo, H. Kodial, P., Bolton, W., Hinzman, L., and Yoshikawa, K. 2005. Effects of Climatic Change in a Sub-Artic Watershed in Alaska, US. In Proceedings: CONAGUA 2005. XX National Water Congress and III Symposium on Water Resources of the Southern Cone (on CD), 11 pp.

Monitoring thermokarst evolution at
Caribou-Poker Creeks Research Watershed

Introduction

In recent years, many researchers have estimated or reported the effects of climate warming in cold regions. The degradation of discontinuous permafrost in sub-artic Alaska has been already reported (Osterkamp and Romanovsky, 1999). The Permafrost Task Force's report, 2003; Hinzman *et al.*, 2004 have pointed out the increasing development of thermokarsts in sub-artic settings. Extensive work on thermokarst has been conducted on the thermal aspects (i.e.: Yoshikawa and Hinzman, 2003; Fraver, 2003, among others). However, detailed studies on morphologic and sediment transport processes on thermokarsts have not been performed. This study focused on the role of sediment transport processes in the spatial and temporal evolutions of a thermokarst located in the Caribou-Poker Creeks Research Watershed (CPCRW). The study was conducted in a thermokarst which development increased markedly after a very high precipitation event in July 2003. According to Burn (1992), thermokarsting process is indicated by slumping along the banks and drunken trees (trees inclined to the ground depressions). These characteristics are clearly visible in the area. This report presents some initial findings and observations on thermokarst evolution and sediment transport. It also explores the possible effects of the accelerated growth of the thermokarst on the local topography.

Study Area and Methods

The thermokarst is located in the CPCRW, which is a tributary to the Chatanika River (Slaughter and Lotspeich, 1977). The area is underlain by discontinuous permafrost. The watershed is reserved to conduct research in sub-artic environments. It was established as research site in 1969. Human activity in the area is restricted to research work. Thus, processes studied there are representative of natural settings. Soil type in the thermokarst area is predominantly silt loam. Vegetation is typically spruce and an organic mat consisting of moss and low growing shrubs (Rieger, et al., 1972). Terrain slope in the area is mild.

Field work in the study site started in March and was carried out to September 2004. Two locations were selected along the thermokarst for discharge measurements and water sampling. One of them was located at the thermokarst water input, namely, "upstream". The other one was located in the central portion of the thermokarst, here defined as "downstream".

The discharge was measured using the volume-by-time method. Water samples were collected in 1000 ml plastic bottles for suspended sediment concentration and grain size distribution analyses. An autosampler, ISCO model 3700, was installed in the downstream site. The autosampler was programmed to take a sample every 6 hs. The same bottle in the instrument was used to collect four consecutive samples. Thus, an integrated daily sample was obtained from

each bottle in the autosampler. The instrument was working during the entire period of its deployment in the field to allow the water sampling during sudden rainfalls which are common in the watershed.

The collected water samples were analyzed in laboratories at the Water and Environmental Research Center (WERC), UAF to determine the suspended sediment concentration and grain size distributions.

Topographical surveys were conducted at the beginning and end of summer of 2004. The first field survey was performed in May after breakup. The second field survey was conducted in the first week of October. Field measurements were taken to determine the lateral and inward thermokarst expansions. The sedimentation of a natural depression, pond-like feature, in the downstream site was monitored over the summer.

Results and Discussion

Figure 1 shows the measured discharges at the upstream and downstream study locations as well as recorded precipitation. Precipitation values plotted on the secondary axis were obtained from the *National Atmospheric Deposition Program (NADP)* rain gauge installed close to the thermokarst site. Measurable discharge into the thermokarst was first observed on April 24, 2004. In general, peak flows were observed the day after a rainfall event indicating a delayed response time at the thermokarst.

During the early part of spring and summer the water supply to the thermokarst was by snow melt and precipitation. By mid summer there was significant discharge even though there was no rainfall. In addition, the discharge at the downstream site was typically lower than the upstream discharge. Both of these factors suggest that groundwater flow is important in the thermokarst area.

The suspended sediment concentration plots for the same locations are shown in Figure 2. High values of suspended sediment concentration were calculated after rainfall events, especially during late May and early June. Available data show that suspended sediment concentration after snowmelt was very small. Maximum sediment concentration, close to 40 mg/g, was measured towards the end of May when the flow path changed from surface water to groundwater. The eroded material from the soil matrix was moved in suspension and deposited in the pond due to the reduction in the sediment transport capacity (i.e.: reduction of flow velocity). Bed sediment deposit thickness in the pond was around 60 cm. At the end of summer, after consolidation and drying, the thickness was approximately 55 cm.
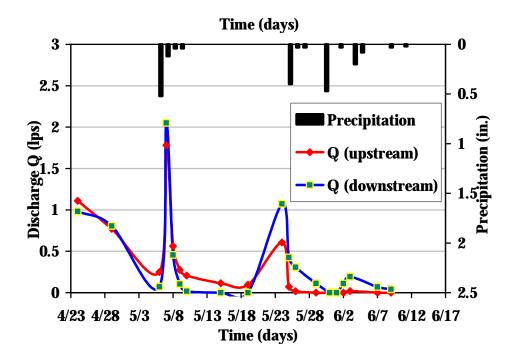
Figure 1. 2004 discharge measurement plots for the upstream and downstream study locations. Discharge ceased towards end of June due to the unusual dry summer. Precipitation data is indicated on the secondary axis.
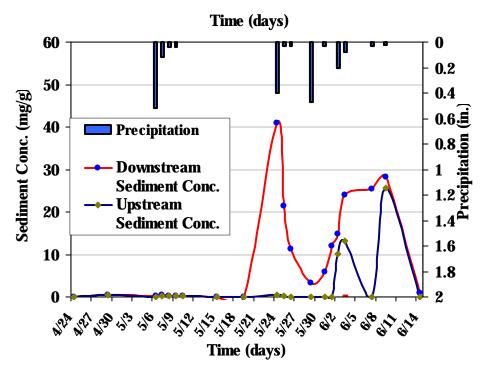

Figure 2. 2004 sediment concentration plots for the upstream and downstream sites. Precipitation data is indicated on the secondary axis.

One of the main factors for the high rate of lateral erosion detected at the upstream site during the field season was due to the combined erosive effects of flowing water and permafrost thawing. This type of erosion along lake and river banks is known as fluvio-thermal erosion (French, 1996).

Drastic morphologic changes were detected in the entire study area. As an example, Figure 3 shows the evolution at the downstream location. Specifically, the figure indicates the sequence of events that were observed at the downstream site. There was significant discharge after breakup (Figure 3(a)) followed by erosion along the banks (Figure 3(b)). Muddy water is clearly noticeable in Figure 3(c). Pond completely filled at the end of summer is shown in Figure 3(d).

Figure 3. Thermokarst evolution at the downstream site. (a) 4/29/2004 photo after snowmelt; (b) 5/15/2004 photo showing erosion; (c) 5/24/2004 photo showing sediment laden flow; (d) 8/13/2004 photo of the sediment bed. Flow direction in all the photographs is from bottom to top.

Results from the particle size analyses are presented in Figure 4. The data indicate that during snowmelt the sediment sizes in suspension were very small compared to sediment in suspension during following periods. The curves progressively shift towards the right, thus suggesting a general increase in the particle size with time. However, mid summer the curve again shifts to the left due to lower flows (i.e.: reduction in sediment transport capacity).

Morphologic changes were calculated through the comparison of topographic surveys. Specifically, the upstream point moved about 2.5 m. Lateral erosion at the downstream site was approximately 0.5 m on both banks.
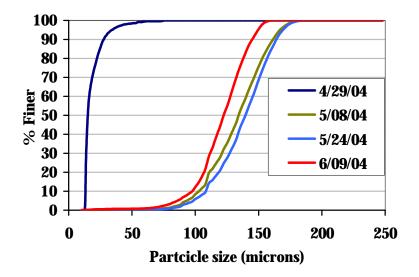
Figure 4. Particle size distribution analyses curves of suspended sediment samples.

Conclusions

The thermokarst site at CPCRW has markedly evolved in the past summer. Main changes are related to lateral and upward bank erosion. Active sedimentation processes in the downstream location allowed a significant volume reduction in the existing pond. Sediment concentration and sediment sizes during the early breakup indicated that in spite of high water discharge, practically no sediment was in suspension. It may be an indication that no sediment is available to be moved during snow melt (i.e.: all sediment is frozen). Climate warming in interior Alaska may lead to additional thermokarsts developing in CPCRW. The thermokarst under study is not likely to develop into a thermokarst lake due to the absence of special conditions like flat topography and high ground-ice content (Kääb and Haeberli, 2001). If there are more warm summers such as during 2004, and sufficient ground ice present in the vicinity, very rapid thermokarst activity may lead to more slumping and undercutting of the banks. Additionally, one can hypothesize that a small stream will form in time, which in turn may ultimately discharge sediment and water into the Caribou creek.

References

Burn, C. (1992). "Canadian Landform Examples – 24: Thermokarst Lakes" *The Canadian Geographer*, 36(1), 81-85

Fraver, M. (2003). "Hydrology of Thermokarst Ponds near Council, Alaska" *M.S. Thesis*, University of Alaska Fairbanks, 106 pp.

French, H. M. (1996). "The Periglacial Environment" 2nd Edition, Longman Group Limited, London, 5.1 – 5.7.4.

Hinzman, L. D., Toniolo, H. A., Yoshikawa, K., and Jones, J. B. (2004). "Thermokarst Development in a Changing Climate" *ACIA International   Symposium on Climate Change in the Arctic*, Oral Session 1: 1.7.

Kääb, A., and Haeberli, W. (2001). "Evolution of a High-mountain Thermokarst Lake in the Swiss Alps" *Arctic, Antarctic and Alpine Research*, 33(4), 385-390.

Osterkamp, T. E., and Romanovsky, V. E. (1999). "Evidence for Warming and Thawing of Discontinuous Permafrost in Alaska" *Permafrost and Periglacial Processes*, 10, 17-37.

Rieger, S., Furbush, C. E., Schoephorster, D. B., Summerfield, H. Jr., and Geiger, L. C., (1972). "Soils of the Caribou-Poker Creeks Research Watershed Interior Alaska" *Tech. Rep. 236*, Hanover, NH: U. S. Army Cold Regions Research and Engineering Laboratory, 11 p.

Slaughter, C. W., and Lotspeich, F. B. (1977). "Caribou-Poker Creeks Research Watershed" *Arctic Bulletin*, 2(10), 183-188.

U.S. Arctic Research Commission Permafrost Task Force. (2003*)* "Climate Change, Permafrost, and Impacts on Civil Infrastructure." *Special Report 01-03*, U.S. Arctic Research Commission, Arlington, Virginia.

Yoshikawa, K., and Hinzman, L. D. (2003). "Shrinking Thermokarst Ponds and Groundwater Dynamics in Discontinuous Permafrost near Council, Alaska" *Permafrost and Periglacial Processes*, 14, 151-160.

Development of Crab Shell Based Biosorbents for Removing Anionic Metal Complexes From Contaminated Water

Basic Information

Title:	Development of Crab Shell Based Biosorbents for Removing Anionic Metal Complexes From Contaminated Water
Project Number:	2004AK26B
Start Date:	3/1/2004
End Date:	3/1/2005
Funding Source:	104B
Congressional District:	AK
Research Category:	Water Quality
Focus Category:	Waste Water, Treatment, None
Descriptors:	biosorption, chitosan, arsenic
Principal Investigators:	Silke Schiewer

Publication

1. Zhang, H..; Schiewer, S. 2005. Arsenic (V) sorption on crab shell based chitosan. In: Proceedings of ASCE EWRI World Water & Environmental Resources Congress, Anchorage, AK, May 15-19 (7 pp.).
2. Zhang, H..; Schiewer, S. 2005. Poster presentation: Arsenic (V) sorption on crab shell based chitosan. In: Proceedings of ASCE EWRI World Water & Environmental Resources Congress, Anchorage, AK, May 15-19.

Problem and research objectives

Mining is one of the major economic activities in Alaska's interior. Mining operations generate leachates from mine tailings containing toxic heavy metals. Due to the large amounts of waste streams to be treated, it is important to develop cost-efficient methods to remove heavy metals from contaminated waters such as tailing leachates.

A particularly cost-effective method for heavy metal removal from waste streams is the emerging process of biosorption. Biosorption is defined the passive uptake of heavy metals by biomass. This process combines the advantages of being, on the one hand, highly efficient at metal removal and, on the other hand, much more cost-effective than comparable techniques such as ion exchange (Volesky 1990). One reason for this cost-effectiveness is that waste products from other industries can be used as biosorbents.
Alaska's Fisheries industry, which is an important economic factor in the coastal regions, produces large quantities of crab shells as waste products. These crab shells contain chitin as one of their main constituents. Chitin/chitosan, which is produced industrially from materials such as crab shells, can be effective at binding heavy metals (Guibal 1999, Mcafee 2001, Navarro 2000), however they are rather costly. Since chitosan contains positively charged amine groups, it can be hypothesized that crab shells will be particularly suitable for removing anionic metal complexes. The current project focuses on utilizing crab shells as low cost biosorbents for the removal of heavy metals from aqueous solutions, for example mine leachates.

The goal of the proposed project was to develop an efficient biosorbent from waste crab shells. The objectives were to
- Optimize the processing methods and conditions (temperature, concentration of reagents) to convert waste crab shells into an efficient biosorbent
- Characterize the resulting biosorbent material
- Test the obtained modified crab shell materials in arsenic biosorption studies
- Compare different crab shell derived materials regarding their sorption capacity.
- Investigate the effect of pH on sorption performance and determine optimal conditions.

Methodology

All experiments used double deionized water (DDI) and ACS reagent grade chemicals. Arsenic stock solution was prepared by dissolving $Na_2HAsO_4 \cdot 7H_2O$ in double deionized water.
a) Preparation of chitin and chitosan

The freeze-dried crab shells were crushed manually. The particle size fraction between 1-2 mm was selected for further processing. According to the method suggested by Muzzarelli (1977), the decalcification was carried out by soaking the crushed crab shells in 50 g/L hydrochloric acid (HCl) at room temperature for 24 hr (8 hr, 3 fold). After that, 5% NaOH solutions were used for a three-fold digestion of about 40 min to remove the proteins. The chitin produced was washed to neutral pH after those reactions. The deacetylation of chitin was achieved by soaking the chitin samples in NaOH solutions of various concentrations ranging from 10% to 40% (w/w) at 121°C in an autoclave for 120 minutes.
b) IR Spectroscopic studies

Fourier transform infrared (FTIR) measurements were carried out as described by Yoshihiro.et al (1996). Accordingly, KBr discs were prepared from dried mixture of about 1 mg of the sample and 100mg of KBr powder. The IR spectrum was recorded on a Thermo IR100 spectrometer. DDA is measured by calculating the ratio of the absorbance of a probe band (PB),

whose intensity changes with DDA with the absorbance of a reference band (RB), whose intensity does not change with DDA. The intensities of the adsorption bands were determined based on the baseline method.

c) Arsenic (V) sorption

The arsenic biosorption was carried out by contacting known quantities of sorbent (1g/L) with arsenic anion solutions within a range from 0.01mM to 2.5 mM at an initial pH value 5. The pH was adjusted manually with HNO_3 or NaOH as required. Biosorption was performed under magnetic agitation at 200 rpm at 20° C for 2 hours. Membrane filters (0.45 μm) were used to separate the sorbents from the equilibrium solution. Arsenic concentrations in the solutions before and after the sorption process were determined by an inductively coupled plasma mass spectrometer (ICP-MS).

d) Titration

Titration of the sorbents was carried out on a Metrohm 719 titrator. The samples were suspended or dissolved in 0.3N HCl solutions, and titrated by 0.1 N NaOH. A curve with 2 inflection points was obtained, from which both the pK_a of the amino group and the amount of surface charge on the sorbent were calculated.

Principal findings and significance

FTIR determination of chemical modification effectiveness (conversion to chitosan).

The main goal of the chemical treatment was to obtain a sorbent with a high content of chitosan, which contains amine groups. Chitosan is obtained by deacetylation of chitin. Therefore the degree of deacetylation (DDA) indicates how efficient the treatment was.

To evaluate the degree of deacetylation, FTIR spectra, which indicate the presence and abundance of functional groups in the tested material, were used. To interpret the FTIR spectrum, the peak of carbonyl stretching in the amide group at 1650 $cm^{-1}$and 1630 $cm^{-1}$was chosen as to indicate the amount of amide groups, and the peak of CO stretching at 1070 was chosen as the reference band to indicate the total amount of monomers as suggested by Duarte et al. (2002).

For a certain source of chitin, the DDA is determined by three factors i.e. base concentration, reaction temperature and reaction time. The results presented in Fig. 1 show a linear relationship between the DDA and base concentration for fixed reaction temperature and reaction time. Sorbents with DDA ranging from 14% to 89% were obtained for adsorption studies.
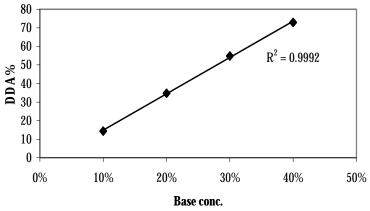

Fig. 1 Influence of base concentration on DDA

Arsenic Adsorption isotherms

The sorption capacities of sorbents with different DDA were evaluated by conducting isotherm studies. The results (Fig. 2) show that the uptake of As (V) increased with an increase of DDA from 10% to 50%, whereas at very high DDA (approximately 90%), the adsorption capacity of the sorbent decreased. This is because DDA determines both the amount and availability of the functional group which can bind As (V). It has been shown （M.L.Duarte et al., 2002） that in the DDA range from 0-80%, the amount of amino groups increases and the crystallinity of the polymer decreases with the increase in DDA, which means that more binding sites are exposed. However, in the very high DDA range (approximately 90%), the As(V) uptake decreases even though the amount of functional groups is increased. This probably occurs because of re-crystallization due to high deacetylation (M.Jaworska et al., 2003). Increased crystallinity may reduce binding site accessibility due to tight packing of chitosan fibers, creating steric hindrance for arsenic. In the present research, the influence of crystallinity on sorbent's adsorption capacity still needs to be confirmed via X-ray diffraction.
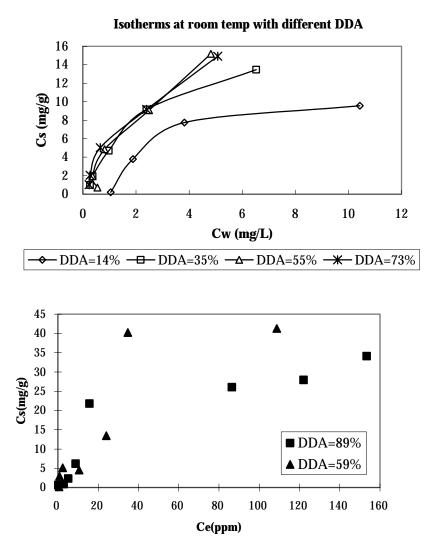

Isotherms at room temp with different DDA

—◇— DDA=14%   —▭— DDA=35%   —△— DDA=55%   —✳— DDA=73%

■ DDA=89%
▲ DDA=59%

Fig. 2. Adsorption isotherms (a) with DDA ranging from 14 – 73% (b) at DDA 59% and 89%

3.2 Optimization of pH

Sorbent with DDA 59% was used to study the change in As(V) sorption capacity with pH. As shown in Fig. 3, the maximum uptake was observed at pH 5, while at both pH 2 and pH 8, the uptake is very low. This difference in uptake can be explained by analyzing the surface charge of sorbent as well as sorbate. The pK_a's for As(V) are 2.2/6.7/11.6 (H_3AsO_4/ $H_2AsO_4^-$/ $HAsO_4^{2-}$). Therefore, at pH above 3 at least approximately 80% of As(V) is in the form of negatively charged species. For chitosan, both the buffer capacity of the amino group and the total surface charge (Fig 4) were calculated from the potentiometric titrations. Since the buffer intensity reaches a maximum at the pK_a, it can be seen from Fig. 4 that the amino group in the sorbent has a pK_a at approximately 6.8. This implies that at pH below 6, most of the amino groups were positively charged. Thus, the maximum uptake is expected in the pH range 3-6, which was confirmed by uptake measurements shown in Figure 3.
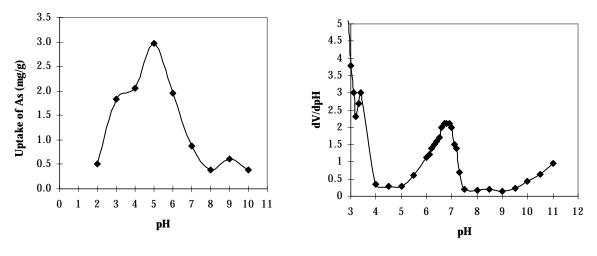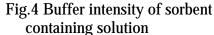

Fig.3 pH influence on As(V) adsorption

Fig.4 Buffer intensity of sorbent containing solution

The amount of charge on the sorbent can be calculated using charge balance calculations:

ENC: $[X] = [OH^-] + [Cl^-] - [Na^+] - [H^+]$

Where X is the charge in equivalent /mol;

Cl^- and H^+ added as HCl;

OH^- and Na^+ are added during titration.

Here $[H^+]$ and $[OH^-]$ are calculated from pH, and $[Na^+]$ as well as $[Cl^-]$ are assumed be same amount as added initially.

Fig.5 shows that at low pH the sorbent is positively charged. However, in addition to amino groups, hydroxyl groups and probably the bridge oxygen, which might also be protonated may also contribute towards the total positive charge. The steep slope of the curve suggests that the weakly bound protons will be released with a slight increase in pH. In the pH range 3.5 to 5.5, only amino groups are protonated, and the total amount of positive charge is almost constant. At even higher pH, the amino group is also gradually deprotonated, and the total charge of sorbent becomes neutral. Therefore, the

surface charge curve helps in understanding the higher uptake of As (V) at pH 5, and decreased uptake at higher pH.
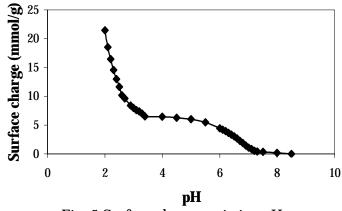

Fig. 5 Surface charge variation pH

Conclusions:

The degree of deacetylation (DDA), a very important factor in determining the amount of functional groups and crystalline character of the sorbent, increases with treatment temperature and NaOH concentration.

The adsorption capacity of the sorbent increases in the DDA range from 10%-80% because of increasing amino group content and reduced crystallinity. However, when the DDA reached 90% or higher, the sorption capacity of the sorbent decreased due to re-crystallization of chitosan.

Arsenate uptake is optimal around pH 5. This can be explained by the magnitude of charge on both sorbent and sorbate, which varies with pH. Below pH 6-7, crab shell chitosan has positively charged amino groups, which can bind arsenic oxyanions. Since arsenate is negatively charged above pH 2-3, it is in the pH range between 3 and 6 that almost all amino groups in chitosan are positively charged the As (V) is negatively charged. This matches well with the observed As uptake between pH 3 and 6, with a maximum around pH 5, suggesting that electrostatic attraction plays an important role in the adsorption process.

The results of this ongoing research show that biosorption of As(V) by crab shell based chitosan is a promising technique to treat the arsenic contamination. Ongoing research focuses on investigating the mechanism of As uptake by modified crab shells.

References:

M.L.Duarte, M.C.Ferreira, M.R.Marvao, Joao Rocha, 2002. An optimized method to determine the degree of acetylation of chitin and chitosan by FTIR spectroscopy, *International Journal of Biological Macromolecules*, Vol. 31, 1-8

Guibal, E.; Dambies, L.; Milot, C.; Roussy, J. (1999). Influence of polymer structural parameters and experimental conditions on metal anion sorption by chitosan. Polym. Int. 48 671-680.

M.Jaworska, K. Sakurai, P.Gaudon, E.Guibal, 2003, Influence of chitosan characteristics on polymer properties. I: Crystallographic Properties, *Polymer International,* Vol.52, 198-205.

Mcafee, B. J., Gould, W. D., Nadeau, J. C., and A.C. A. Da Costa. 2001. Biosorption of metal ions using chitosan, chitin, and biomass of *Rhizopus oryzae*. Sep. Sci. Technol.: 36(14): 3207-3222.

R.A.A.Muzzarelli, *Chitin*, Pergamon Press, Oxford, 1973.

Navarro, R.R. and Tatsumi, K. (2001) Improved performance of a chitosan-based adsorbent for the sequestration of some transition metals. *Wat. Sci. Technol.* 43, No. 11, 9-16

Volesky, B. (1990) Removal and recovery of heavy metals by biosorption. In: Volesky, B. (Ed.), *Biosorption of Heavy Metals*, CRC Press, Boca Raton, FL, 7-43.

Infiltration in Coarse Soil and Formation of Infiltration Ice

Basic Information

Title:	Infiltration in Coarse Soil and Formation of Infiltration Ice
Project Number:	2004AK29B
Start Date:	3/1/2004
End Date:	3/1/2005
Funding Source:	104B
Congressional District:	AK
Research Category:	Ground-water Flow and Transport
Focus Category:	Climatological Processes, Geomorphological Processes, Hydrology
Descriptors:	Drainage, Seasonally Frozen Soil, Permafrost, Infiltration, Infiltration Ice
Principal Investigators:	David L. Barnes, Yuri Shur

Publication

Investigation of the Formation of Pore Ice in Coarse Grained Soils

Overview

Numerous studies of ice formation in soils are focused on fine-grained soils freezing in closed or open systems mainly in attempt to describe frost heave impact on structures. While the characteristics of the accumulation of ice in fine grain soil have been thoroughly studied, the formation of ice in coarse grain soil has not been investigated. Freezing of fine grain soils is accompanied by movement of water to the freezing front and formation of stratified ice layers. Such temperature gradient induced soil-water migration is not the case for coarse-grained soils with small amount of fines (soil particles with diameters less than 0.075mm). Also, differing water retention characteristics in comparison to fine grain soil and mechanisms of moisture transfer suggest that the nature of pore ice formation in coarse grain soil is different than in fine grain soil. Understanding the nature of ice formation in this type of soil and the soil characteristics that control the depth at which the pore space becomes saturated with ice is important to assessment and cleanup of contaminated coarse grained soil to include naturally deposited soils as well as engineered soils such as the base coarse of air strips, roadways, and gravel foundations in northern, alpine, and Arctic climates. In addition, others are investigating the use of permeable reactive barriers to control the migration of surface and subsurface contamination in cold climates. Design of these barriers requires an understanding of where ice is likely to form in the pore space and if preferential channels for flow will form due to the presence of ice. Furthermore, in the area of geotechnical engineering, knowledge of pore ice formation in coarse graded base soil materials is required to reduce the impact of roadway weakening during thawing. As accumulated ice near the top of base soils directly underneath the paved surface thaws high pore water pressures reduce the strength of base soils causing failures in the paved surface.

Drainage of liquids through frozen soils is limited by the formation and presence of ice in the porous matrix in comparison to similar unfrozen soil. As water added to the soil by rain events or by melting snow drains through frozen soil, a fraction of the water will be retained in pore space and eventually freeze. Ultimately, with repeated infiltration of water, pore space will become saturated with ice restricting any additional infiltration of water. The infiltration of other liquids such as non-aqueous phase liquids (for example petroleum) accidentally released to the ground surface will also be impacted by the presence of ice in the pore space. Proper assessment and cleanup of these impacted regions first requires a better understanding of how pore ice changes the characteristics of porous media. The overall objective of this project was to quantify the factors controlling the formation of pore ice in coarse grained soil.

Laboratory Methodology

The infiltration studies were conducted in a walk-in cold room to ensure a homogeneous temperature distribution through the columns. The columns were constructed of acrylic to facilitate a visual interpretation of the results. The mesh at the bottom of the column has a screen size of 1.5mm. The setup is shown in Figure 1.
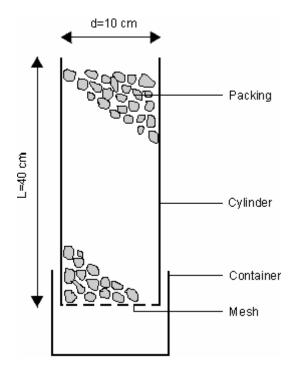
Figure 1: Experimental setup of the column studies

In each test, melt water at $0\,^{\circ}C$ was introduced at the top of the column and allowed to infiltrate and freeze. If the water made it all the way through the column, the permeant was collected in a container and allowed to freeze before the next introduction of melt water was made. To decrease the possibility of inducing a convective current in the column melt water was left in the container below the column and allowed to freeze before the next introduction of melt water. Between each introduction of melt water the column and the container was weighed to establish the partitioning of the permeant. The whole setup was also enclosed in a loose plastic wrapping to minimize the amount of sublimation of ice out of the column. The parameters tested in the column studies were the soil gradation, temperature, volume of water added by infiltration, compaction, and initial soil moisture content and the layout of the tests are shown in Table 1.

Table 1: Test schedule

Test	Soil Type	Temperature
A	Gravel (large –100% passing 25mm)/dry	$-10\,^{\circ}C$
B	Gravel (pea –100% passing 6.25mm)/dry	$-10\,^{\circ}C$
C	Graded surface course /dry /compacted	Room Temperature
D	Graded surface course /dry /compacted	$-2\,^{\circ}C$, $-5\,^{\circ}C$
E	Graded surface course /dry /uncompacted	$-10\,^{\circ}C$
F	Graded surface course with fines (< 75µm) removed /dry /compacted	$-5\,^{\circ}C$
G	Graded surface course /initial moisture contents of 0%, 4.5% and 9% /compacted	$-5\,^{\circ}C$

Results and Discussion

The results from the tests can best be described in a series of figures. A description of how ice forms in a poorly graded soil (singular grain size) as opposed to a well graded material is provided in Figure 2. In well graded material, the existence of small dimensioned pore space created by the presence of varied sized soil grains creates dead end pores as water is retained in these spaces by capillary forces freezes. The result of the creation of dead end pores is ice saturation in the top few centimeters of the column. Conversely, a poorly graded coarse grained soil will have relatively larger dimensions pore space resulting in drainage of the melt water until the latent heat is lost or there is a change in soil gradation. An additional factor contributing to blockage of draining melt water is air entrapment in the near ice saturated pore space. The existence of these often large volumes of entrapped air is shown in Figure 3.
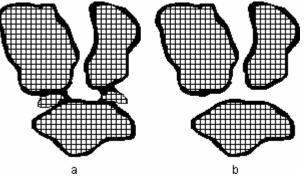

a   b

Figure 2: Comparison of pore ice formation in coarse grained soils with (a) and without (b) the presence of smaller particles. Cross hatched areas represent soil grains and the solid areas represent water held by capillary forces. The scenario shown in (a) represents the creation of a dead-end pore with minimal pore ice content in comparison to the scenario shown in (b) where pore channels remain open to flow. Further additions of water to the pore space shown in (a) will result in the pore becoming either filled with ice or entrapped air.

Figure 3: Large volumes of entrapped air form because of dead end pores

In poorly graded soil or in relatively large dimensioned pore spaces, melt water rapidly freezes to soil grain surfaces changing the pore dimensions of the coarse grained soil. Eventually pores become blocked as the pore dimensions are reduced such that melt water can be retained by capillary forces. This process is illustrated in Figure 4.
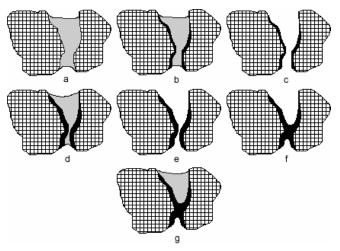

Figure 4: The hypothetical freezing of coarse grained soils from infiltration of melt water. In (a) the pore is filled with fluid, the fluid rapid freezes to the pore walls (b) and then drains (c). Successive infiltration causes additional freezing to the pore walls (d) and (e) until the pore has been closed off (f). Thus the pore-throat has become a dead end (g).

Gradation changes from fine grained soil to coarse grained soils are of interest due to the development of capillary breaks and the restriction of further water drainage through the soil horizon. In a frozen soil, ice will form in the soil above the capillary break. This effect was seeing in our test as water was retained in the mesh openings at the bottom of the column as shown in Figure 5.
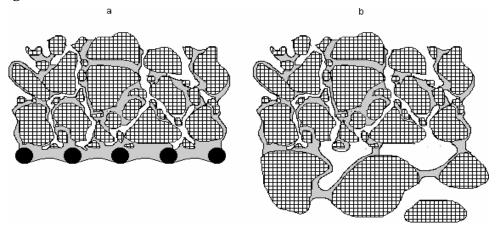

Figure 5: Water held by a capillary break freezes at the interface. In (a) the laboratory experiment is shown were water is infiltrated at the top, advances to the capillary break and is unable to pass as the pressure head is not great enough to infiltrate the pore space below. The water freezes at this point and subsequent additions of melt water will pond on top of the impermeable layer. This can be likened to the real world situation in (b) were a gradation change takes place, as in the case of a surface course on top of a base course.

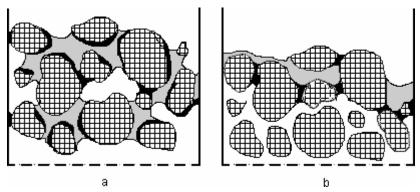Compaction also plays a very important role in ice formation; this relationship is summarized in Figure 6.

Figure 6: In compacted sample in (b) the pore throats have become much smaller than those in (a). The rapid freezing process described previously occur much more readily and therefore the impermeable layer forms higher up in the sample.

Conclusions

The freezing mechanism of infiltration ice is an important issue with regards to engineered coarse grained soils. Infiltrated melt water rapid freezes to the soil grain boundaries, decreasing the pore throat diameter and increasing the resistance to flow. The addition of relatively finer particles (not necessarily clay and silt) to a coarse grained soil also decrease the average pore throat diameter and drastically changes the location of the initial impermeable ice layer. The sub-zero temperature of the soil does not greatly affect the freezing rate or the location of the ice layer, as the latent heat of water is orders of magnitude higher than its specific heat. The compaction of the soil also affects the formation of the ice layer. In compacted soils the small particles are forced in between the bigger particles, decreasing the average pore throat diameter. The initial frozen moisture content greatly influences the pore space available for flow.

The application of this theoretical work can be shown in engineered coarse grained porous media such as permeable reactive barriers (PRBs) and road beds. In permeable reactive barriers care should be taken to reduce the possibility of flow channeling, which would reduce the effectiveness of the PRB. Moreover, the possibility of a capillary break between the engineered barrier soil and the surrounding soil should be reduced. Such a break would also allow water to freeze at the PRB boundary and further reduce its efficiency. In road beds the fine material in the surface coarse is largely responsible for the retention of water and the subsequent problems with rutting and thaw settlement.

Information Transfer Program

Student Support

Student Support					
Category	Section 104 Base Grant	Section 104 RCGP Award	NIWR-USGS Internship	Supplemental Awards	Total
Undergraduate	0	0	0	0	0
Masters	3	0	0	0	3
Ph.D.	1	0	0	0	1
Post-Doc.	0	0	0	0	0
Total	4	0	0	0	4

Notable Awards and Achievements

Results from Barnes and Shur's project, "Infiltration in Coarse Soil and Formation of Infiltration Ice," have made it possible to win significant funding for larger projects from the National Science Foundation and Alaska Department of Conservation, to develope collaborations with the Australia Antarctic Division to apply our results to permeable reactive barrier development in the Antarctic and Arctic these collaborations, in addition to furthering research in this area, will support additional students and and international student exchange.

Publications from Prior Projects

1. 2002AK1B ("Investigation of Immiscible Fluid Movement Through Frozen Porous Media") - Articles in Refereed Scientific Journals - Barnes, D.L., S.M. Wolfe, and D.M. Filler. 2004. Equilibrium Distribution of Petroleum Hydrocarbons in Freezing Ground. Polar Record, 40 no. 3: 245-251.
2. 2002AK5B ("Investigation of Fouling in Membrane Bioreactors for Wastewater Treatment") - Articles in Refereed Scientific Journals - Psoch, C.; Schiewer, S. 2004. Critical Flux aspects of air sparging and backflushing in membrane bioreactors. Desalination 175 (1) 61-71.